

Supporting Information

Peptide valence-induced breaks in plasmonic coupling

Yu-Ci Chang,^{a,‡} Zhicheng Jin,^{b,‡} Ke Li,^c Jiajing Zhou,^b Wonjun Yim,^a Justin Yeung,^d Yong Cheng,^b Maurice Retout,^b Matthew N. Creyer,^b Pavla Fajtová,^e Tengyu He,^a Xi Chen,^f Anthony J. O'Donoghue,^e and Jesse V. Jokerst^{a,b,g*}

^a Materials Science and Engineering Program, University of California San Diego, La Jolla, CA 92093, United States.

^b Department of NanoEngineering, University of California San Diego, La Jolla, CA 92093, United States.

^c Institute of Materials Research and Engineering, Agency for Science, Technology and Research, Singapore 138634, Singapore.

^d Department of Bioengineering, University of California San Diego, La Jolla, CA 92093, United States.

^e Skaggs School of Pharmacy and Pharmaceutical Sciences, University of California San Diego, La Jolla, CA 92093, United States.

^f School of Materials Science and Engineering, Nanyang Technological University, Singapore 639798, Singapore.

^g Department of Radiology, University of California San Diego, La Jolla, CA 92093, United States.

[‡] These authors contributed to this work equally.

*Corresponding author's email: jjokerst@ucsd.edu (J.V.J.)

Table of Contents

1.	Materials.....	3
2.	Materials synthesis and instrumentations	4
2.1	Peptide synthesis	4
2.2	Gold nanoparticles characterization	5
3.	Electronic structure calculations	5
4.	One-pot assays	5
5.	Peptide cleavage by trypsin.....	5
6.	References	6
Table S1. Molecular weight (M.W.) of the intact and fragmented peptides.....		8
Table S2. Operation windows of R2 and K2 peptide in Tris buffer.....		9
Figure S1. Structures of DPPS, BSPP, and TPPTS.....		10
Figure S2. CCC calculation for simple metallic cations.		11
Figure S3. HPLC and ESI-MS data of synthesized $G_{5-x}R_x$ peptides.		12
Figure S4. AuNP properties, CCC calculation for $G_{5-x}R_x$ peptides, and the operation window of K2 peptide.		13
Figure S5. Systems in initial structures for MD simulations.		14
Figure S6. HPLC and ESI-MS data of synthesized peptides and their cleaved fragments.....		15
Figure S7. The structure of R2 peptide.....		16
Figure S8. Operation windows calculation for ligand-AuNPs and peptides.		17
Figure S9. LoD calculation for M^{PrO} , inhibitor potency, and HPLC of trypsin cleavage.		18
Figure S10. The colorimetric map of the sensing kit.		19

1. Materials

Triphenylphosphine-3,3',3''-trisulfonic acid trisodium salt hydrate (TPPTS, 85%) was purchased from Beantown Chemical (Hudson, NH). Bis(*p*-sulfonatophenyl)phenylphosphine dihydrate dipotassium salt (BSPP, 97%), gold(III) chloride trihydrate ($\text{HAuCl}_4 \cdot 3\text{H}_2\text{O}$, >99.9%), sodium citrate tribasic dihydrate (>99%), copper(II) chloride (99%), Trizma[®] base (>99.9%), Trizma[®] hydrochloride (>90%), trifluoroacetic acid (TFA, HPLC grade, >99%), piperidine (ReagentPlus[®], 99%), trypsin (Tp), thrombin (Tb), hemoglobin (Hgb), and bovine serum albumin (BSA) were purchased from Sigma Aldrich (St Louis, MO). *N,N*-diisopropylethylamine (DIPEA, >99%), sodium diphenylphosphinobenzene-3-sulfonate (DPPS, >90%), and triisopropylsilane (TIPS, >98%) were purchased from Tokyo Chemical Industry Co., Ltd. (TCI). Sodium chloride (certified ACS), potassium chloride (certified ACS), calcium chloride (certified ACS), erbium(III) chloride, iron(III) chloride hexahydrate (97%), ferrous chloride tetrahydrate (certified crystalline), and magnesium chloride hexahydrate (certified ACS) were purchased from Fisher Scientific International, Inc. (Hampton, NH). Gadolinium(III) chloride was purchased from GFS Chemicals, Inc. (Powell, OH). Fmoc-protected amino acids, hexafluorophosphate benzotriazole tetramethyl uranium (HBTU), and Fmoc-Rink amide MBHA resin (0.67 mmol/g, 100-150 mesh) were purchased from AAPPTec, LLC (Louisville, KY).

The recombinant main protease (M^{pro} without His-tag) of SARS-CoV-2 was expressed and purified as outlined previously.¹ The M^{pro} was stored in 20 mM Tris-HCl (pH 8.0), with 150 mM NaCl, 1 mM DTT, and 5 % glycerol at $-80\text{ }^\circ\text{C}$. M^{pro} inhibitor GC376 (507.53 g/mol) was purchased from Selleckchem. Organic solvents including *N,N*-dimethylformamide (DMF, sequencing grade), acetonitrile (ACN, HPLC grade), ethyl ether (certified ACS), and methylene chloride (DCM, certified ACS) were also from Fisher Scientific International, Inc. (Hampton, NH). Ultrapure water (18 M Ω -cm) was obtained from a Milli-Q Academic water purification system (Millipore Corp., Billerica, MA). TEM grids (formvar/carbon 300 mesh Cu) were purchased from Ted Pella (Redding, CA). Automation compatible syringe filters (hydrophilic PTFE, 0.45 μm) were from MilliporeSigma (St. Louis, MO). Polyester swabs (25-806 2PD) were purchased from Puritan Medical (Guilford, ME). Glassware and stir bars were cleaned with aqua regia ($\text{HCl}:\text{HNO}_3=3:1$ by volume) and boiling water before use.

2. Materials synthesis and instrumentations

2.1 Peptide synthesis

Peptides were synthesized using an automated Eclipse™ peptide synthesizer (AAPPTec, Louisville, KY) through standard solid phase Fmoc synthesis on Rink-amide resin. Peptides were lyophilized in a FreeZone Plus 2.5 freeze dry system (Labconco Corp., Kansas, MO). All peptides were chain assembled by Fmoc-SPPS (solid-phase peptide synthesis) on Rink-amide resin (0.67 mmol/g, 200 mg) using the Fmoc-peptide synthesizer. Amino acid couplings were performed with Fmoc-amino acid (5 equiv.), 0.15 M HBTU in DMF (5 equiv.), and 0.3 M DIPEA (10 equiv.). The number of coupling cycles followed the sequence analyzer built in the peptide synthesizer. Finished peptides on the resin were transferred into a syringe filter and washed with five rounds of DCM (~ 5 mL each round). Then, peptides were cleaved from the resin using a cleavage cocktail (3 mL) that contained TFA (88% v/v), TIPS (2% v/v), phenol (5% w/v), and H₂O (5% v/v). Resins were stirred with the cleavage cocktail for 2.5 hours. After the cleavage, the resin was filtered into 50 mL centrifuge tube. Crude peptides were precipitated with cold ether (30 mL) and centrifuged under 7,000 g for 3 mins, then removing the supernatant. The ether washing step and the centrifugation step were processed for 3 times. Then, suspending crude peptides in 50% ACN/H₂O (6 mL) and lyophilizing.

Peptides were purified by the reversed phase HPLC, characterized by the ESI-MS, aliquoted and stored in dry conditions at -20 °C for use. The absorbance at 205 nm of aqueous peptide sample was measured using the nanodrop spectrophotometer to quantify the peptide concentration. In the standard plot of optical absorbance vs. mass concentration, the slope of the linear regression line was indicated as, $\epsilon_{205} \sim 74.6 \text{ mL}\cdot\text{mg}^{-1} \text{ cm}^{-1}$ (water or Tris buffer was used).

Peptide purification was carried out using a Shimadzu LC-40 HPLC system equipped with a LC-40D solvent delivery module, photodiode array detector SPD-M40, and degassing unit DGU-403. The sample was dissolved in 50% ACN/H₂O, applied on a Zorbax 300 BS, C18 column (5 μm , 9.4×250 mm) from Agilent, and eluted at 1.5 mL/min with a 40 min gradient from 10% to 95% of acetonitrile in water (with 0.05% TFA). Preparative injections were monitored at 190, 220, and 254 nm.

Peptide synthesis and cleavage was confirmed using electrospray ionization mass spectrometry (ESI-MS) via the Micromass Quattro Ultima mass spectrometer in the Molecular MS Facility (MMSF) at Chemistry and Biochemistry Department, UC San Diego. ESI-MS samples were prepared in a 50% MeOH/H₂O mixture. Peptide concentration was determined using a NanoDrop™ One UV-vis spectrophotometer (Thermo Fisher Scientific, Waltham, MA).

2.2 Gold nanoparticles characterization

The optical absorption measurements were collected using a hybrid multi-mode microplate reader (Synergy™ H1 model, BioTek Instruments, Inc.) in a clear 96-well plate. The dynamic light scattering (DLS) and zeta potential measurements were carried out using a Zetasizer Nano ZS90 (Malvern Panalytical, Inc.). Transmission electron microscopy (TEM) images of the Au colloids were acquired using a JEOL 1200 EX II operated at 80 kV. The TEM grids were prepared by drop casting samples in water (4 μ L) followed by natural drying. Photographic images were taken by smartphone in a lightbox of white background.

3. Electronic structure calculations

To determine the partial charge on the atomic sites of TPPTS and peptides, the B3LYP hybrid functional² and def2TZVP basis set³ were applied to optimize the molecules and calculate the wavefunctions using the Gaussian09 package.⁴ The DFT-D3 dispersion functional⁵ was incorporated to take the Van der Waals interactions into consideration. With the optimized wavefunctions, the Multiwfn⁶ package was then used to calculate the RESP charge.

4. One-pot assays

In the one-pot assay, the particle aggregation and the enzyme cleavage occur *in situ*. The parent R2 peptide ($c_{\text{final}} = 5 \mu\text{M}$) was mixed with TPPTS-AuNPs (100 μ L, 3.6 nM) solution for 10 min incubation under room temperature to reach the stable aggregation state. Then, M^{pro} enzymes and Tris buffer/ exhaled breath condensate/saliva of desirable amount were added to each R2-AuNPs solution. The total volume of each tube was 120 μ L. Next, new mixtures were transferred into a 96-well plate and incubated in 37 °C for 2 hours. The absorbance at 600 and 520 nm of above mixtures were readout in the microplate reader at 37 °C every 1 min for 2 hours at the same time. The ratiometric signal ($\lambda_{600/520}$) at 2 hour was extracted for analyses. At least two replicates of each experiment were made.

5. Peptide cleavage by trypsin

To investigate whether arginine in the R2 peptide can be cleaved by trypsin, we made the peptide-enzyme mixture. The peptide solution (110 μ L, $\sim 2 \text{ mg/mL}$) in Tris buffer (20 mM, pH 8.0, with 150 mM NaCl, 1 mM DTT) was incubated with the trypsin ($\sim 163 \text{ nM}$) at 37 °C overnight. The mixture was then applied on a Shim-pack GIS, C18, analytical column (5 μ m, 4.6 \times 100 mm) from Agilent, and eluted at 1 mL/min with a 40 min gradient from 10% to 95% acetonitrile. Preparative injections were monitored at 190, 220, and 254 nm. All fractions were collected, and the molecular weight was determined using the ESI mass spectrometer.

6. References

1. D. M. Mellott, C. T. Tseng, A. Drelich, P. Fajtova, B. C. Chenna, D. H. Kostomiris, J. Hsu, J. Zhu, Z. W. Taylor, K. I. Kocurek, V. Tat, A. Katzfuss, L. Li, M. A. Giardini, D. Skinner, K. Hirata, M. C. Yoon, S. Beck, A. F. Carlin, A. E. Clark, L. Beretta, D. Maneval, V. Hook, F. Frueh, B. L. Hurst, H. Wang, F. M. Raushel, A. J. O'Donoghue, J. L. de Siqueira-Neto, T. D. Meek and J. H. McKerrow, *ACS Chem. Biol.*, 2021, **16**, 642-650.
2. P. J. Stephens, F. J. Devlin, C. F. Chabalowski and M. J. Frisch, *The Journal of Physical Chemistry*, 1994, **98**, 11623-11627.
3. F. Weigend and R. Ahlrichs, *Physical Chemistry Chemical Physics*, 2005, **7**, 3297-3305.
4. M. J. Frisch, G. W. Trucks, H. B. Schlegel, G. E. Scuseria, M. A. Robb, J. R. Cheeseman, G. Scalmani, V. Barone, B. Mennucci, G. A. Petersson, H. Nakatsuji, M. Caricato, X. Li, H. P. Hratchian, A. F. Izmaylov, J. Bloino, G. Zheng, J. L. Sonnenberg, M. Hada, M. Ehara, K. Toyota, R. Fukuda, J. Hasegawa, M. Ishida, T. Nakajima, Y. Honda, O. Kitao, H. Nakai, T. Vreven, J. A. Montgomery, J. E. Peralta, F. Ogliaro, M. Bearpark, J. J. Heyd, E. Brothers, K. N. Kudin, V. N. Staroverov, R. Kobayashi, J. Normand, K. Raghavachari, A. Rendell, J. C. Burant, S. S. Iyengar, J. Tomasi, M. Cossi, N. Rega, J. M. Millam, M. Klene, J. E. Knox, J. B. Cross, V. Bakken, C. Adamo, J. Jaramillo, R. Gomperts, R. E. Stratmann, O. Yazyev, A. J. Austin, R. Cammi, C. Pomelli, J. W. Ochterski, R. L. Martin, K. Morokuma, V. G. Zakrzewski, G. A. Voth, P. Salvador, J. J. Dannenberg, S. Dapprich, A. D. Daniels, Ö. Farkas, J. B. Foresman, J. V. Ortiz, J. Cioslowski and D. J. Fox, *Bull. Chem. Soc. Jpn.*, 2009, **85**, 679-686.
5. S. Grimme, S. Ehrlich and L. Goerigk, *Journal of Computational Chemistry*, 2011, **32**, 1456-1465.
6. T. Lu and F. Chen, *Journal of Computational Chemistry*, 2012, **33**, 580-592.
7. D. R. Hurst, M. A. Schwartz, Y. Jin, M. A. Ghaffari, P. Kozarekar, J. Cao and Q. X. Sang, *Biochem. J.*, 2005, **392**, 527-536.
8. P. J. Henderson, *Biochem. J.*, 1972, **127**, 321-333.

Table and Figures (Supporting Information)

Table S1. Molecular weight (M.W.) of the intact and fragmented peptides.

Name	Peptide Sequence	M.W. (g·mol ⁻¹)
G ₅ R ₀	GGGGG	302.1
G ₄ R ₁	GGGGR	401.2
G ₃ R ₂	RGGGR	500.3
G ₂ R ₃	RGGRR	599.4
G ₁ R ₄	RRGRR	698.5
G ₀ R ₅	RRRRR	797.5
R0	PASTSAVLQ↓SGFPAS	1417.7
N-terminal fragment of R0	PASTSAVLQ	872.5
C-terminal fragment of R0	SGFPAS	563.3
R2	RTSAVLQ↓SGFRG	1276.7
N-terminal fragment of R2	RTSAVLQ	773.4
C-terminal fragment of R2	SGFRG	521.3
R4	RGRTSAVLQ↓SGFRG R	1645.9
N-terminal fragment of R4	RGRTSAVLQ	986.6
C-terminal fragment of R4	SGFRGR	677.4
r2	TSAVLQ↓SGFRGR	1276.7
N-terminal fragment of r2	TSAVLQ	617.3
N-terminal fragment of r2 (without T)	SAVLQ	516.3
C-terminal fragment of r2	SGFRGR	677.4
K2	KTSAVLQ↓SGFKG	1220.7
N-terminal fragment of K2	KTSAVLQ	745.4
C-terminal fragment of K2	SGFKG	493.3
N-terminal fragment of R2 cleaved by trypsin	RTSAVLQSGFR	1220.7
C-terminal fragment of R2 cleaved by trypsin	TSAVLQSGFRG	1120.6

All the peptides contain free N-terminus (–NH₂) and amidated C-terminus (–CONH₂).

Table S2. Operation windows of R2 and K2 peptide in Tris buffer.

Name	Operation Window (μM)		
	DPPS-Au	BSPP-Au	TPPTS-Au
R2	0.1 - 4.6	3.8 - 24.2	2.5 - 63.3
K2	-	-	5.0 - 65.1

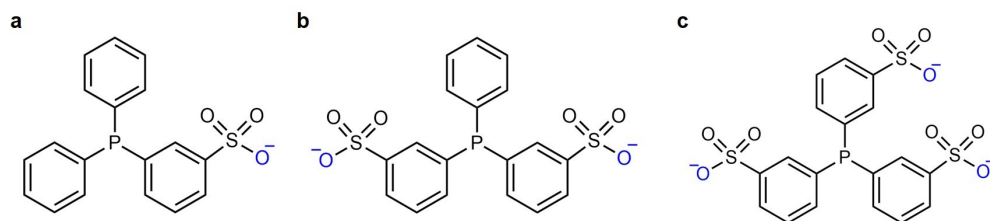


Figure S1. Structures of DPPS, BSPP, and TPPTS.

(a) Diphenylphosphinobenzene sulfonate (DPPS) with one sulfonate group. (b) Bis(*p*-sulfonatophenyl)phenylphosphine (BSPP) with two sulfonate groups. (c) Triphenylphosphine-3,3,3-trisulfonate (TPPTS) with three sulfonate groups.

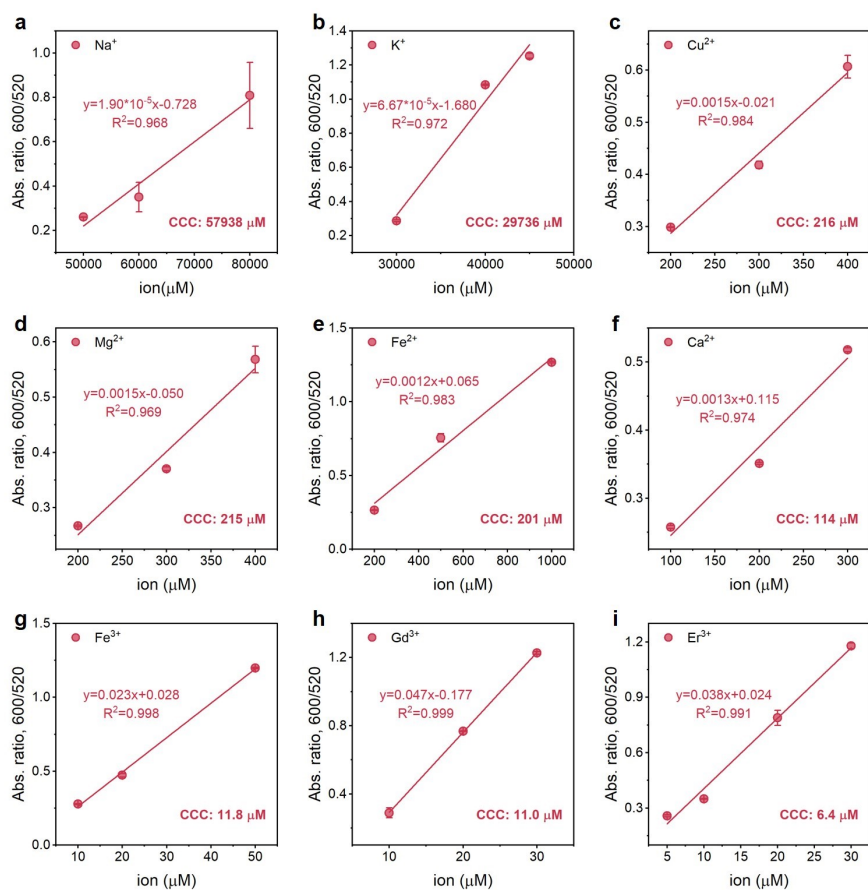


Figure S2. CCC calculation for simple metallic cations.

Linear regions used to calculate the critical coagulation concentration (CCC) of (a) Na⁺, (b) K⁺, (c) Cu²⁺, (d) Mg²⁺, (e) Fe²⁺, (f) Ca²⁺, (g) Fe³⁺, (h) Gd³⁺, and (i) Er³⁺. Measurements were performed in duplicates. Error bar = standard deviation.

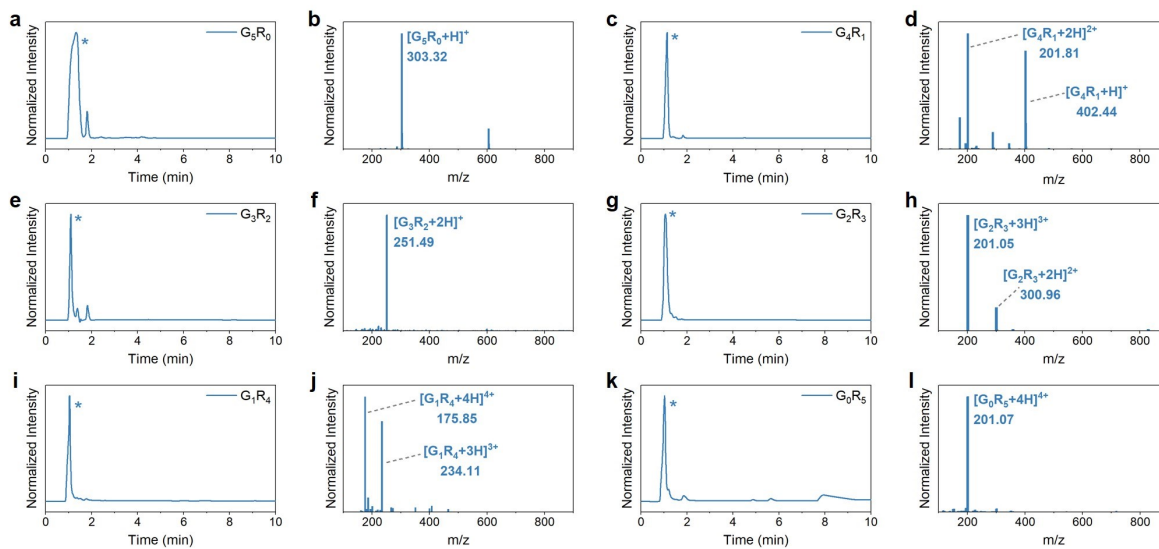


Figure S3. HPLC and ESI-MS data of synthesized $G_{5-x}R_x$ peptides.

(a,c,e,g,i,k) HPLC data collected from G_5R_0 , G_4R_1 , G_3R_2 , G_2R_3 , G_1R_4 , G_0R_5 , respectively.

(b,d,f,h,j,l) ESI-MS data collected from G_5R_0 , G_4R_1 , G_3R_2 , G_2R_3 , G_1R_4 , G_0R_5 , respectively.

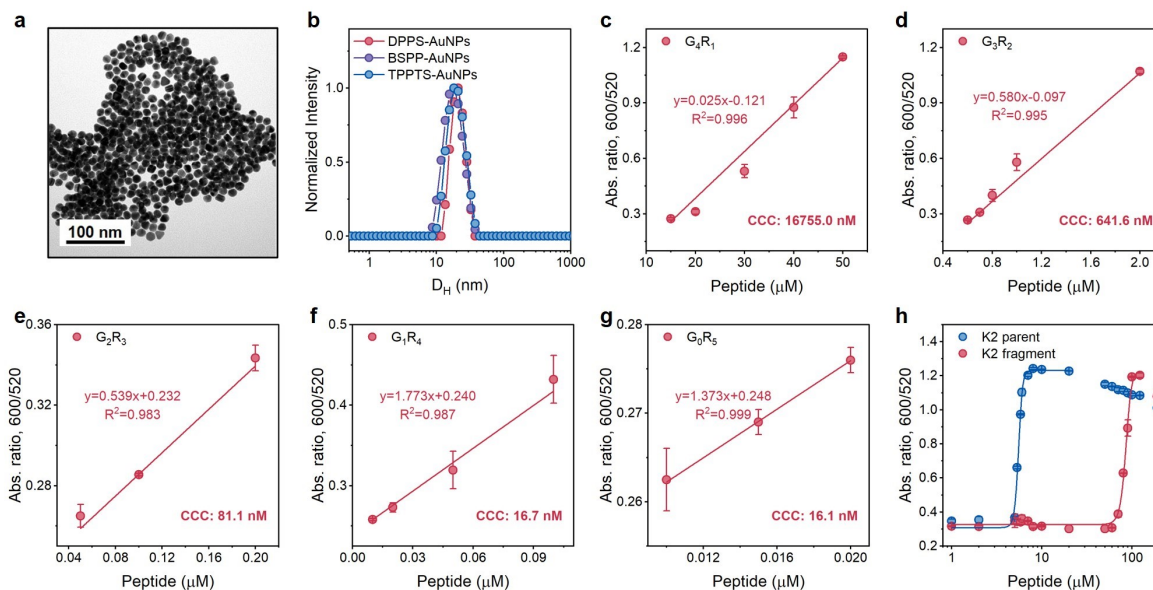


Figure S4. AuNP properties, CCC calculation for G_{5-x}R_x peptides, and the operation window of K2 peptide.

(a) Transmission electron microscopy (TEM) image of free TPPTS-AuNPs. (b) Dynamic light scattering (DLS) profiles of DPPS-AuNPs ($D_H = 19.8$ nm, PDI=0.17, red), BSPP- AuNPs ($D_H = 19.2$ nm, PDI= 0.29, purple), and TPPTS-AuNPs ($D_H = 18.9$ nm, PDI=0.13, blue). (c-g) Linear regions used to calculate CCC of G₄R₁, G₃R₂, G₂R₃, G₁R₄, and G₀R₅. Measurements were performed in duplicates (error bars = standard deviation). (h) The operation windows of M^{pro} sensors based on K2 peptide. The data was collected at readout time = 10 min. Error bar = standard deviation.

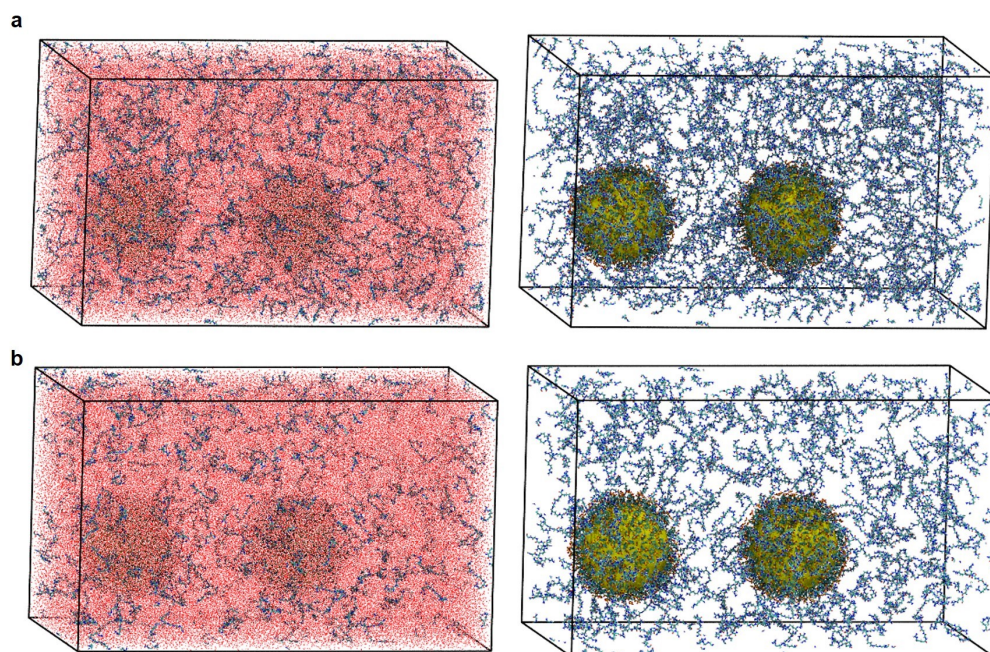


Figure S5. Systems in initial structures for MD simulations.

(a) System of G_4R_1 peptide and TPPTS-AuNPs. The left panel shows pink water molecules, and the right panel shows without water molecules. (b) System of G_3R_2 peptide and TPPTS-AuNPs. The left panel shows pink water molecules, and the right panel shows without water molecules.

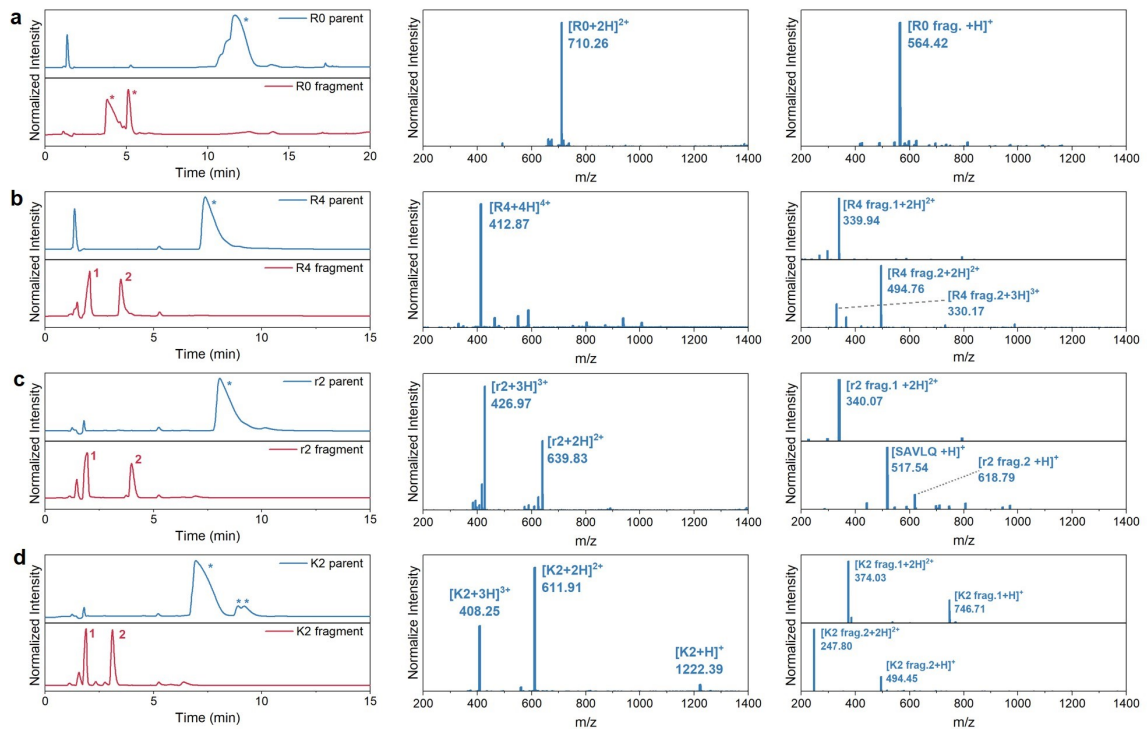


Figure S6. HPLC and ESI-MS data of synthesized peptides and their cleaved fragments.

HPLC data are shown in the left panel, and ESI-MS data of parent peptides and corresponding fragments are shown in the middle and right panel, respectively. (a-d) Data collected from R0, R4, r2, and K2 peptide with M^{pro}, respectively; cleavage after Gln (Q). Peaks with * represent parent peptide product; Peaks with 1 or 2 represent fragments from the cleaved peptide.

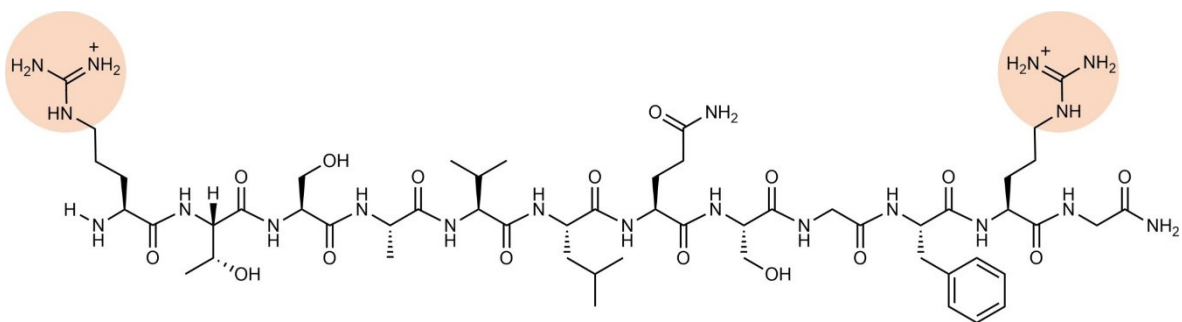


Figure S7. The structure of R2 peptide.

Orange colors represent positively charged domains.

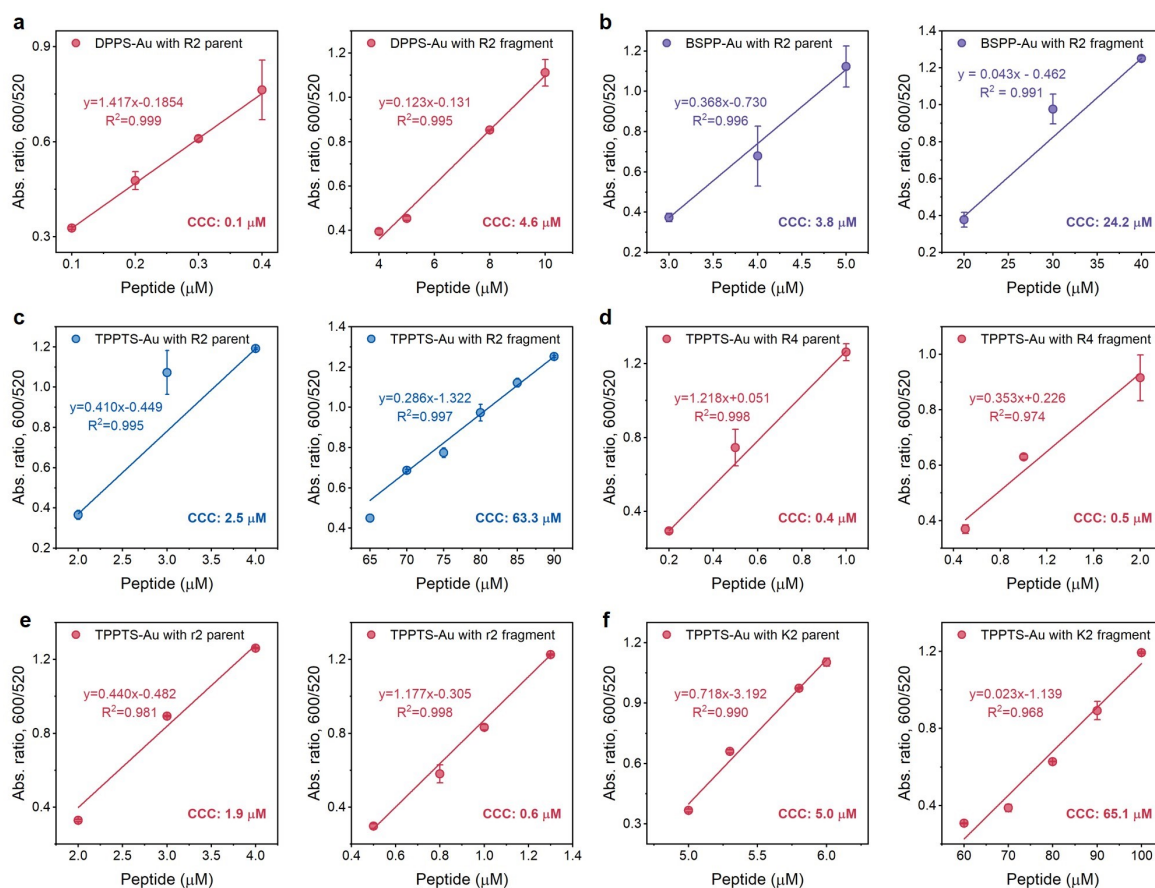


Figure S8. Operation windows calculation for ligand-AuNPs and peptides.

Linear regions used to calculate operation windows in different AuNPs or peptides. Measurements were performed in at least duplicates (error bars = standard deviation). (a-c) R2 parents/fragments with (a) DPPS-AuNPs, (b) BSPP-AuNPs, and (c) TPPTS-AuNPs. (d-f) TPPTS-AuNPs titrated by (d) R4 parents/fragments, (e) r2 parents/fragments, and (f) K2 parents/fragments.

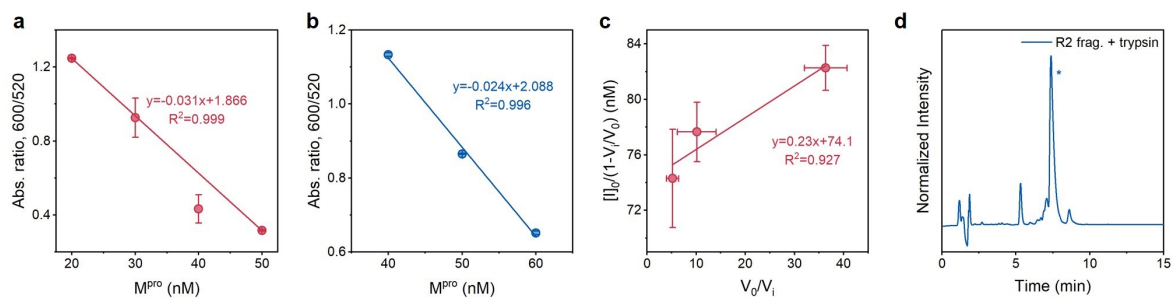


Figure S9. LoD calculation for M^{Pro} , inhibitor potency, and HPLC of trypsin cleavage.

Linear regions used to calculate limit of detection (LoD) for M^{Pro} in (a) two-step reaction in **Figure 4h** and (b) one-pot assay in **Figure 4j**. Measurements were performed in at least duplicates (error bars = standard deviation). (c) Henderson equation, $[I]_0/(1-V_i/V_0) = [E]_0 + K_{i(app.)} \times (V_0/V_i)$, was applied to resolve the apparent inhibitor dissociation constant, $K_{i(app.)} = 0.23$ nM, and active enzyme concentration, $[E]_0 = 74.1$ nM. The $IC_{50} \sim 37.3$ nM is derived from, $IC_{50} = K_{i(app.)} + [E]_0/2$.^{7,8} Note that the inverse of fractional velocity, V_0/V_i , is extracted from the absorbance ratio at 10 min in **Figure 5a**. (d) HPLC data collected from R2 peptide with trypsin; cleavage after Arg (R). Peaks with * represent cleaved product.

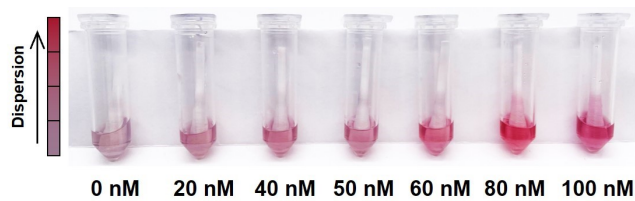


Figure S10. The colorimetric map of the sensing kit.

The LoD of the sensing kit is estimated to be 20 nM after 15 hr incubation. Redispersed TPPTS-AuNPs appear pink or red depending on the concentration of M^{pro} , while the color of TPPTS-AuNPs solution without M^{pro} addition remains purple.